HHS Public Access

Author manuscript

*Cell Rep*. Author manuscript; available in PMC 2016 September 22.

Published in final edited form as:

*Cell Rep*. 2016 September 13; 16(11): 3062–3074. doi:10.1016/j.celrep.2016.08.029.

# An integrative analysis of the InR/PI3K/Akt network identifies the dynamic response to Insulin signaling

**Arunachalam Vinayagam**[1,2,#], **Meghana M. Kulkarni**[1,7,#], **Richelle Sopko**[1], **Xiaoyun Sun**[2], **Yanhui Hu**[1,3], **Ankita Nand**[3,4], **Christians Villalta**[1], **Ahmadali Moghimi**[1], **Xuemei Yang**[5], **Stephanie E. Mohr**[1,3], **Pengyu Hong**[2], **John Asara**[5], and **Norbert Perrimon**[1,6,*]

[1]Department of Genetics, Harvard Medical School, 77 Avenue Louis Pasteur, Boston, MA 02115, USA

[2]Department of Computer Science, Volen Center for Complex Systems, Brandeis University, Waltham, MA 02454, USA

[3]Drosophila RNAi Screening Center, Department of Genetics, Harvard Medical School, 77 Avenue Louis Pasteur, Boston, MA 02115, USA

[4]Bioinformatics program, Northeastern University, 360 Huntington Avenue, Boston, MA 02115, USA

[5]Division of Signal Transduction, Beth Israel Deaconess Medical Center, Boston, MA 02115, USA

[6]Howard Hughes Medical Institute, 77 Avenue Louis Pasteur, Boston, MA 02115, USA

## Summary

Insulin regulates an essential conserved signaling pathway affecting growth, proliferation and metabolism. To expand our understanding of the insulin pathway, we combine biochemical, genetic and computational approaches to build a comprehensive Drosophila InR/PI3K/Akt network. First, we map the dynamic protein-protein interaction network surrounding the insulin core pathway using bait-prey interactions connecting 566 proteins. Combining RNA interference screening and phospho-specific antibodies, we find that 47% of interacting proteins affect pathway activity, and using quantitative phosphoproteomics, we demonstrate that ~10% of interacting proteins are regulated by insulin stimulation at the level of phosphorylation. Next, we integrate

*To whom correspondence should be addressed: perrimon@receptor.med.harvard.edu.

[7]Present address: Oncology Bioscience, Astrazeneca, 35 Gatehouse Drive, Waltham MA 02451, USA

[#]Authors contributed equally



**Authors Contributions**

M.K., A.V. and N.P. conceived and designed the project. AP-MS dataset: M.K. and J.A. designed the experiments, M.K., C.V. and X.Y performed experiments, A.V. designed the computational analysis, A.V., M.K., X.S., A.N. and P.H analyzed datasets. RNAi dataset: M.K. and S.E.M designed the experiments, M.K. and A.M performed experiments, A.V. designed the computational analysis, A.V., M.K., and Y.H. analyzed the dataset. Phosphoproteome dataset: R.S. and M.K. designed and performed the experiments, A.V., R.S. and M.K. designed and performed the analysis. A.V. designed and performed the integrative and protein-complex analysis. M.K designed and performed the validation experiments. N.P supervised the study. A.V., M.K and N.P wrote manuscript. All authors contributed to manuscript preparation.

Competing interests: The authors declare that they have no competing interests.

these orthogonal datasets to characterize the structure and dynamics of the insulin network at the level of protein complexes, and validate our method by identifying regulatory roles for the Protein Phosphatase 2A (PP2A) and Reptin-Pontin chromatin-remodeling complexes as negative and positive regulators of ribosome biogenesis, respectively. Altogether, our study represents a comprehensive resource for study of the evolutionary conserved insulin network.

## Graphical Abstract

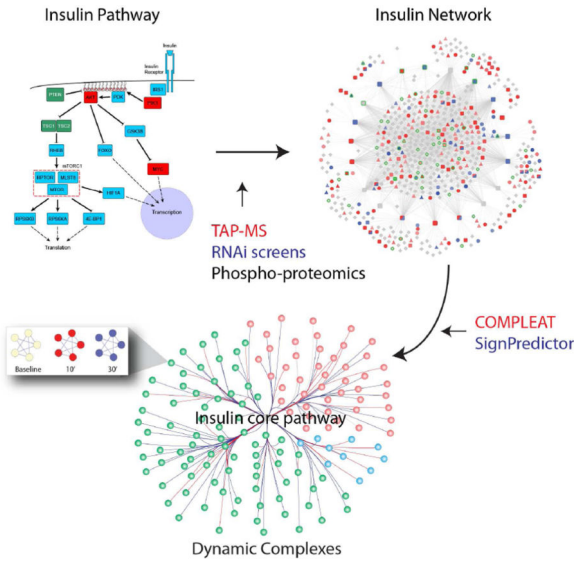


## Introduction

The insulin signaling pathway is highly conserved across all metazoans. In *Drosophila* and mammalian systems, insulin signaling regulates growth during development and in response to a variety of environmental cues such as nutrient availability, intracellular energy levels, hypoxia, osmotic stress, and DNA damage (Reiling and Sabatini, 2006). Regulation of growth occurs through the control of biological processes ranging from general metabolism, protein and lipid biosynthesis, glucose uptake, energy utilization and production, to cell survival, growth and proliferation. Given the plethora of processes modulated by insulin signaling, it is not surprising that a variety of extrinsic and intrinsic factors directly impinge upon this pathway. Further, its fundamental role in cellular and organismal homeostasis is reflected by the fact that dysregulated signaling can lead to a range of systemic disorders including diabetes, obesity, inflammation, cancer, hypertension, high levels of cholesterol and other lipids, heart disease, kidney disease, female infertility and neurodegeneration (White, 2003). Insulin also contributes to the regulation of lifespan (Clancy et al., 2001).

Insulin binds to the extracellular domain of its cognate InR receptor tyrosine kinase (RTK) to initiate a series of intracellular phosphorylation events. Upon insulin binding, the InR is activated through tyrosine autophosphorylation and it phosphorylates several proteins in the cytoplasm, including the InR substrate (IRS) that functions as a docking protein for SH3-domain-containing signaling molecules responsible for the next steps in the signaling cascade. InR signaling recruits two major pathways, the Phosphoinositide 3- kinase (PI3K)

pathway, which mediates the metabolic effects of insulin, and the mitogen-activated protein kinase (MAPK) pathway, which mediates the mitogenic effects of insulin in concert with the PI3K pathway.

The insulin signaling pathway is highly evolutionarily conserved and many components are well characterized both at the molecular and biochemical levels. In *Drosophila* more than twenty proteins have been assigned as core insulin signaling pathway components (Teleman, 2010). To expand our understanding of the structure and function of the insulin pathway, we decided to build a comprehensive map of the insulin network as done in recent years for a number of other *Drosophila* different pathways, using proteomic and functional genomic studies (Friedman et al., 2011; Kwon et al., 2013). While small-scale networks (with approximately 50 proteins) for the insulin pathway have been built (Glatter et al., 2011; Humphrey et al., 2015; Humphrey et al., 2013), a comprehensive network is not yet available. Thus, we used three orthogonal technologies, Affinity-purification mass spectrometry (AP-MS) for mapping protein-protein interaction (PPI), RNA interference (RNAi) to functionally characterize the interactors, and phosphoproteomic data to identify targets of the pathway. To capture signaling dynamics, we mapped the network at three different time points following insulin stimulation. Next, we annotated the network by organizing interacting partners as protein complexes and characterized their relationship with the pathway (activation/inhibition). This integrated network was systematically mined to identify protein complexes that are essential for insulin signaling and candidate complexes validated *in vitro* and *in viv*o. Altogether, our study represents a comprehensive resource of the evolutionary conserved insulin network.

## Results

We used S2R+ cells as a model system to build the *Drosophila* insulin network (InsulinNet) (Figure 1). InsulinNet components were identified and characterized by: 1) mapping a PPI network centered on 20 canonical pathway members using AP-MS (InsulinNet-PPI); 2) functional characterization of InsulinNet proteins by RNAi using pAKT and pERK as readouts (InsulinNet-RNAi); and 3) identification of pathway targets using global phosphoproteome measurements (InsulinNet-Phospho). To capture the dynamics of the insulin network, data was collected at three time points, baseline (without insulin treatment), and after insulin stimulation for 10 or 30 minutes. The time points were chosen based on the pathway activity by measuring pAKT and pERK levels (Figure S1). The pathway activity is low at baseline, peaks at 10 minutes and returns close to normal by 30 minutes due to feedback regulation.

### InR/PI3K/Akt protein-protein interaction network

To map the dynamic PPI network surrounding the insulin core pathway, we selected 20 well-characterized, conserved canonical components of the pathway as baits and performed tandem affinity purification (TAP) assays in *Drosophila* S2R+ cells (Table S1). TAP-tagged proteins were expressed in S2R+ cells and lysates prepared at baseline (unstimulated cells) or after stimulation with insulin for 10 or 30 minutes. All experiments were performed using three biological replicates, thus representing altogether 201 samples for mass spectrometry

characterization (Figure 2A). In total, we identified an unfiltered network of 16,893 interactions (bait-prey relationships) connecting 20 bait proteins with prey proteins (Table S1). Note that some of the bait proteins are also identified as prey proteins due to intimate interaction between the canonical components.

We applied the Significance Analysis of Interactome (SAINT) (Choi et al., 2011) algorithm to filter out non-specific interactors from the raw TAP-MS data. We compiled lists of literature curated PPIs, positive reference set (PRS), and non-specific interaction, negative reference set (RRS), to assess the performance of the SAINT score and to chose a cut-off value (see Experimental Procedures and Table S1). Our evaluation shows that SAINT score is robust in distinguishing true interactions from non-specific interactions (Area Under Curve of 0.94 in the ROC plot) (Figure S2) and we chose a SAINT score cutoff of 0.95 (false positive rate < 4%). Known InR-PI3K-Akt signaling pathway interactions (Figure 2B, Table S1), including those between the adaptor IRS/chico and InR, the PI3K subunits p110 (PI3K92E) and p60 (PI3K21B), the Tumor suppressor complex subunits Tsc2/gigas and Tsc1, and the downstream translational regulators 4E-BP/Thor and eIF-4E, are identified above the SAINT score cutoff of 0.95.

Using a SAINT cutoff of 0.95, we generated a filtered Insulin PPI Network (InsulinNet-PPI) of 1807 interactions between 554 proteins (Figure 2C, 2D and Table S1). More than 10% of the interactions present in InsulinNet-PPI are supported by the literature, either from *Drosophila* and/or interologs mapped from human, mouse, *C. elegans*, or yeast (see Experimental Procedures and Table S1) (Figure 2E). This overlap is significantly higher than random expectation (4 fold higher). Interestingly, more PPIs identified at 10 minutes overlap with the literature and are supported by multiple evidences compared to the other two time points.

InsulinNet-PPI consists of 554 preys that correspond to 274 proteins identified at baseline, in addition to 242 and 430 proteins identified at 10 and 30 minutes, respectively (Figure 2C). Among the 554 prey proteins, 100 proteins interact at all three time points (baseline, 10 and 30 minutes), 192 proteins interact at two, and 262 proteins interact at a single time point. Sixty-six percent of prey proteins (365) interact with two or more baits and the remaining 34% (189 proteins) interact with single baits (Figure 2D). Interestingly, while most individual bait proteins interact with distinct prey proteins at baseline, they tend to share common prey proteins after stimulation with insulin, suggesting that pathway components only assemble in response to the stimulus (Figure 2F). Similarly, module-based clustering indicates that canonical pathway components close together in the signaling pathway share more interacting proteins with each other than with components further upstream or downstream in the pathway (Figure 2F). These observations further validate the quality of InsulinNet-PPI.

To functionally characterize InsulinNet-PPI, we performed Gene Ontology (GO) enrichment analysis (Boyle et al., 2004) (Figure 2G and Table S2). The functional categories enriched among the proteins that interact with all three time points capture most of the known roles of the insulin pathway, including the regulation of cell proliferation, cell size, aging, autophagy and apoptosis (Reiling and Sabatini, 2006; Teleman, 2010). The interactors specific to the 10

minutes condition are enriched for functions such as translation, ribosome biogenesis, cell cycle and RNA processing, which are key functions regulated by the pathway. Almost 96% (531 out of 554 prey proteins) of the interacting proteins identified are conserved in human (Table S2). These conserved prey proteins are implicated in a wide range of human diseases including different cancer types and Type II diabetes (Table S2), demonstrating the relevance of our network for extrapolation to human diseases.

We systematically compared InsulinNet-PPI with other relevant published *Drosophila* PPI networks and calculated the significance of overlapping interactions. First, we compared InsulinNet-PPI with the InR/Tor PPI network consisting of 97 interactions connecting 58 proteins (Glatter et al., 2011). This network was generated in *Drosophila* Kc167 cell lines using 15 canonical components as bait proteins for AP-MS experiments. Although, only 10 out of 20 InsulinNet-PPI baits overlap with the InR/Tor PPI network, the analysis shows significant overlap at the interaction level (23 out of 51 InR/Tor interactions overlap with InsulinNet-PPI; P-value < 0.0001) (Figure 2H and Table S1). Next, we compared our InsulinNet-PPI with a *Drosophila* AP-MS network generated from 3488 individual pull-down experiments (DPiM) (Guruharsha et al., 2011). For the comparative analysis, we selected 1312 PPIs from DPiM that involve 6 overlapping bait proteins shared by DPiM and InsulinNet-PPI and found significant overlap (219 out of 1312 PPIs) between these networks (P-value < 0.0001) (Figure 2H, Table S1 and Table S1). Finally, we compared InsulinNet-PPI with the *Drosophila* MAPK PPI network (Friedman et al., 2011) for which our InsulinNet-PPI shares one bait (InR); we found significant overlap (7 overlapping PPIs; P-value < 0.0001) (Figure 2H, Table S1 and Table S1). Extending the comparative network analysis by including published *Drosophila* PPIs and inferred interactions reveals 192 interactions from InsulinNet-PPI is supported by one or more evidences (see Experimental Procedures and Table S1), further validating the InsulinNet-PPI in terms of relevant PPIs. Finally, we created a web tool, InsulinNet (http://fgr.hms.harvard.edu/InsulinNetwork/), to interactively query and access InsulinNet-PPI data (see details in Experimental Procedures).

## Functional genomic screens to identify regulators of the insulin pathway

To systematically characterize InsulinNet-PPI pathway components, we interrogated by RNAi the function of components of the network using phospho-specific antibodies against Akt and ERK as readouts for pathway activity (see Experimental Procedures). Specifically, we performed six independent RNAi screens in S2R+ cells, measuring pAkt and pERK levels at three conditions (baseline, 10 minutes and 30 minutes insulin treatment) (Figure 3A). We excluded ribosomal proteins and screened almost 90% of the InsulinNet-PPI (480 out of 554) components. To improve the robustness of the RNAi screens, more than 78% of the genes (376 out of 480) were tested with multiple RNAi reagents (independent amplicon designs), including 114 genes (23.7%) that were tested with three or more RNAi reagents in triplicates. We computed the fold change of pERK and pAKT levels compared to controls and identified genes with median log2fold change ≥ 0.5 and ≤ −0.5 as negative and positive regulators of the pathway, respectively (see Experimental Procedures, dataset referred to as InsulinNet-RNAi).

Core components of the pathway scored in the RNAi screens, indicating the robustness of the assays (Table S3 and Figure S3). In particular, as expected from previous studies (Kockel et al., 2010), *InR* and *Pi3K92E* scored as positive regulators while *Pten* and *S6k* scored as negative regulators of pAkt. In addition, we also identified *corkscrew* (*csw*) and *Gap1* as positive and negative regulators of pERK, respectively (Friedman and Perrimon, 2006). In total, 47% of the genes that were tested (226 out of 480) were identified as regulators of pAkt or pERK or both, at baseline or following stimulus (Figure 3A and 3B, Table S3). 42% of the hits regulate only pAkt, 32.3% regulate only pERK, and the remaining 21.7% regulate both (Figure 3B). Of the pAkt regulators, the majority of the hits (115 out of 144) are negative regulators with most of them (65%) scoring at baseline (Figure 3A and Table S3). Positive regulators of pAkt were primarily identified after 10 minutes insulin treatment (30 out of 34). Only 13.8% (20 out of 144) of the hits regulate pAkt at more than one time point and three (*shu, Arc1* and *26–29-p*) were identified as both positive and negative regulators depending on the stimulus condition. We observed a similar tendency for pERK regulators including: more negative regulators scoring at baseline (106 out of 131 hits); 87% of all positive regulators scoring at 10 minutes; and 16% regulating pERK in more than one condition. These results illustrate the need to screen at both baseline and following stimulation to efficiently identify positive and negative regulators of the pathway.

Among the hits that regulate both pAkt and pERK, 9 genes have opposite effects on the two readouts (serving as a positive regulator of pAkt and negative regulator of pERK, or vice-versa). For instance, as previously shown in worm (Hopper, 2006), Csw, a protein tyrosine phosphatase and a core component of MAPK pathway, negatively regulates pAkt and positively regulates pERK. Similarly, we identified Pp2A-29B, a regulatory subunit of the PP2A serine/threonine protein phosphatase, as a positive regulator of pAkt and a negative regulator of pERK. Other genes in this category are: *Hel25E, CG6686, eIF5B, Mi-2, CG42724, CG6227*, and *deltaCOP*. Functional enrichment analysis reveals distinct functions for positive and negative regulators of pAkt and pERK (Figure 3C and Table S3). Common regulators of pAkt and pERK are enriched for insulin signaling related function such as cell cycle and RNA splicing.

Next, we compared our InsulinNet-RNAi dataset with other relevant published RNAi screens available from GenomeRNAi (Schmidt et al., 2013). 15% (34 out of 226) of the InsulinNet-RNAi hits are unique (not reported as hits in other screens) and only 2 genes are frequent hitters (see Experimental Procedures). Next, we compared InsulinNet-RNAi to genome-wide pERK regulator screens (Friedman and Perrimon, 2006) and identified 50 common regulators (P-value < 0.0001). Further, 147 additional regulators were present in InsulinNet-RNAi only and 92 genes previously identified in genome-wide pERK screens were not present in InsulinNet-RNAi, probably reflecting differences in stimulation conditions, cell lines and amplicon design. Finally, since ribosome biogenesis is regulated by insulin signaling, we compared InsulinNet-RNAi with a previous genome-wide screen for regulators of nucleolar size (Neumuller et al., 2013). Significantly, 36 genes were in common between InsulinNet-RNAi and the nucleolar size screen (P-value < 0.0001).

Comparing InsulinNet-RNAi and InsulinNet-PPI revealed that the Tsc complex alone interacts with 36.7% of the RNAi hits (21 with Tsc1, 31 with Gigas (Gig)/Tsc2, and 31 with

both) (Figure 3D and Table S3). 58.5% of the proteins interacting with Pten were hits following knockdown by RNAi (the most for any bait) and the bait with the lowest number of interactors scoring in RNAi screens, Melt, was still highly significant at 22.2%. Strikingly, core components of the Akt pathway interact with almost equal number of pAkt and pERK regulators (Figure 3D), revealing the extent of cross talk between the Akt and MAPK pathways. Only in the case of Akt interactors, we observe a moderate difference with 21 components regulating pAkt, 12 regulating pERK and 8 regulating both. Comparing InsulinNet-RNAi with the dynamics of InsulinNet-PPI reveals that pAkt regulators identified following 10 minutes insulin show significant overlap with the physical interaction data (Figure 3E). Furthermore, we identified 8 proteins that specifically associate as well as regulate pAkt levels at 10 minutes after stimulus, suggesting a potential mechanism through which these proteins regulate the pathway (Figure 3E).

## Quantitative phosphoproteomics to identify targets of insulin signaling

To identify targets of insulin signaling, we systematically investigated insulin-induced phosphorylation using quantitative phosphoproteomics. The phosphoproteome of S2R+ cells were analyzed at the same three conditions: baseline, 10 and 30 minutes insulin stimulus. In total we identified 46,483 phosphopeptides from which we localized 3038 unique phosphosites with near certainty (see Experimental Procedures, Table S4). To identify dynamic sites, we normalized the intensities of 10 and 30 minutes to baseline. Sites with significant fold-changes compared to baseline were selected as insulin responsive dynamic phosphosites ($-0.5 <= \log2\text{fold change} >= 0.5$).

We identified 266 insulin responsive dynamic phosphosites from 191 proteins and refer to this subset as InsulinNet-Phospho (Table S4). The phosphosites from InsulinNet-Phospho are classified as “increase”, “early-increase”, “late-increase”, “decrease” “early-decrease” and “late-decrease” based on their dynamic profiles (Figure 4A). The phosphosites of canonical components increase in response to insulin, including the phosphorylation of InR (Y1549 and Y1550), chico (Y860), Pi3K92E (Y138) and raptor (S1091). In total, we categorized 84, 48 and 44 phosphosites into increase, earlyincrease and late-increase classes, respectively (Table S4). Together, these represent 66% of all phosphosites (176 out of 266) changing in response to insulin. On the other end, 22, 49 and 19 phosphosites fell into decrease, early-decrease and late-decrease classes, respectively. Among the decreasing phosphosites, more than half (49 out of 90 sites) are in the early-decrease class that only transiently decreases at 10 minutes after stimulus.

We observed distinct GO functional enrichment for the different dynamic classes (Figure 4B). For instance, the increase class shows enrichment for insulin-regulated functions such as positive regulation of cell size and growth (P-value < 0.001). Interestingly, biological processes such as cell differentiation are enriched in the early-increase class, whereas the negative regulators of cell differentiation are enriched in the early-decrease class. Similarly, increase and early decrease classes show enrichment for processes such as cell cycle.

To identify the potential upstream kinases modulating InsulinNet-phospho, we performed motif enrichment analysis using the MotifX algorithm (Chou and Schwartz, 2011). Motif enrichment analysis reveals that the Akt/S6k consensus motif is significantly enriched

among all classes of increase phosphorylation, implying that Akt1 and/or downstream S6k are active throughout the duration of the treatment (Figure 4C and Table S4). We also observe significant enrichment of proline-directed kinase motifs among early and late increase classes suggesting these sites might be regulated through Cyclin-dependent kinases (CDK) or ERK. Next, we used the Netphorest algorithm (Miller et al., 2008) that uses an atlas of consensus sequence motifs to predict kinase-substrate relationships. Current version of NetPhorest only covers linear motifs for 179 kinases and we are using the kinase-substrate predictions only as suggestive evidence. The analysis revealed that 160 out of 266 dynamic sites are potential targets of canonical pathway kinases, including 60 candidate Akt1 targets and 107 candidate S6k targets (Figure 4D and Table S4). Comparison with a mammalian phosphoproteomic dataset revealed 22.5% of phosphoproteins in the InsulinNet-Phospho are also targets of mTOR complex in human and mouse datasets (Hsu et al., 2011) (Figure 4E and Table S4). Such motif enrichment and comparative analyses show high quality of the InsulinNet-Phospho dataset.

Next, we systematically compared the overlap between InsulinNet-PPI and InsulinNet-Phospho and identified 52 dynamic phosphoproteins physically interacting with the core components of the pathway (Figure 4F and Table S5). Of those 52 proteins, 18 are hits from RNAi screening (part of the InsulinNet-RNAi). Interestingly, the non-RNAi hits are significantly enriched for InsulinNet-PPI (Figure 4G and Table S4). These results suggest that RNAi screening and phosphoproteomics capture different aspects of insulin signaling (see Discussion). Note that even our unfiltered PPI network (with no SAINT score cutoff) shows significant overlap with InsulinNet-Phospho (101 out of 191 proteins) (Figure 4F, Figure 4G and Table S4). Such integrative analysis suggest potential targets of the pathway, for instance, phosphorylation of Pp2A-29B S139 increases in response to insulin stimulus and it has a S6k/Akt consensus motif. Further, PPI data suggests that it physically interacts with the Akt1, indicating that Pp2A-29B could be a potential Akt1 substrate. Finally, we identified 13 proteins, including eIF4G from InsulinNet-Phospho, which also overlap with InsulinNet-PPI and mTOR targets, suggesting that these proteins are involved in insulin signaling (Figure 4H).

## Integrated Insulin signaling network

We combined the InsulinNet-PPI, InsulinNet-RNAi and InsulinNet-Phospho datasets to build an integrative insulin signaling network (InsulinNet) (Figure 5A, 5B and Table S5). 18 proteins in the network overlap within all three datasets, this includes three proteins from the core pathway (InR, chico and Tsc1). Thirty-four proteins comprising the PPI network and their phosphosites are dynamically regulated by the insulin stimulus, including Pi3K92E. Another 208 proteins are part of the PPI network and were identified as regulators of the pathway in RNAi screens. Almost 46% of the proteins in the InsulinNet are validated by two or more orthogonal assays, demonstrating the quality and plenitude of the data.

## Structure and dynamics of the insulin network

To gain further insights into the structure and dynamics of InsulinNet, we applied Protein Complex Enrichment Analysis Tool (COMPLEAT) (Vinayagam et al., 2013) to organize the network into protein complexes (Figure 6A). COMPLEAT identifies protein complexes

enriched in a given high-throughput dataset using a comprehensive protein complex resource. We applied COMPLEAT to identify protein complexes that are either stably or dynamically associated with the insulin pathway. Note, for the COMPLEAT analysis we used unfiltered InsulinNet-PPI (with no SAINT score cutoff) with modified spectral count values as the input (see Experimental Procedures). To identify stably associated protein complexes, we analyzed all three networks (baseline, 10 and 30 minutes) individually and the complexes that are significant (based on COMPLEAT P-values) in all three time points were considered as stably associated protein complexes. In total, 548 protein complexes were considered stably associated (Table S6).

We normalized the modified spectral count values of 10 and 30 minutes data with baseline (computed log2 fold-change values) to identify the dynamic protein complexes that either associate or dissociate with the core pathway. COMPLEAT analysis of 10 and 30 minutes networks were performed individually and the results combined to identify dynamic protein complexes (Figure 6B and 6C). In total, we categorized 282 dynamic complexes belonging to 7 different dynamic classes (Table S6). Forty-one protein complexes significantly associated with the core pathway both at 10 minutes and 30 minutes and we refer to this class as “association complexes”. Similarly, 3 complexes, including Wave-2 complex, are dissociated both at 10 and 30 minutes and we refer these as “dissociation complexes”. We identified 47 protein complexes that associate only at 10 minutes (“early association”) and 6 complexes that dissociate only at 10 minutes (“early dissociation”). Similarly, we identified 144 complexes that associate only at 30 minutes (“late association”) and 39 complexes that dissociate only at 30 minutes (“late dissociation”). We also found two protein complexes related to translational elongation that associate at 10 minutes and dissociate at 30 minutes (“early association and late dissociation” complexes).

Among those complexes we identified as either stably associated or dynamically assembled, 17% (143) are curated in the literature as belonging to those specific protein complexes, and have at least one high-confidence interaction connecting them to the core pathway. This includes 83 stably associated complexes and 60 dynamic complexes, and the remaining are predicted complexes from the COMPLEAT resource (Figure 6D and Table S6). We found that 15 out of the 143 complexes are involved in chromatin remodeling; these include complexes from all four families of chromatin remodeling complexes (SWI/SNF, NURF, NuRD and INO80).

Next, we applied SignPredictor tool (Vinayagam et al., 2014) to characterize the activation/inhibition relationships between the core pathway and interacting complexes (Figure 6A and Table S6). SignPredictor predicts the activation/inhibition relationship between the interacting proteins based on phenotypic signatures from RNAi screens. We have extended this framework to predict the relationship between protein complexes and a pathway (see Experimental Procedures). We used 6 RNAi screens generated in this study and 49 published RNAi screens to construct phenotype signatures. Our analysis reveals that 99 of 143 protein complexes have positive relationships with the insulin pathway (either activate or activated by the pathway) while 36 protein complexes have negative relationships (either inhibit or inhibited by the pathway) (Figure 6D). Note that for 8 protein complexes we could not predict activation/inhibition relationships. We found a negative association between

complexes, including Wave-2 complex, Arp2/3 complex and different protein phosphatase 2A (PP2A) complexes, and the pathway, correlating with a dissociation of the complex in response to stimulus.

## Functional characterization of protein complexes regulating insulin signaling

We focused on characterizing the functionality of the PP2A complex in relation to insulin signaling. PP2A is a heterotrimeric complex, consisting of the serine-threonine phosphatase catalytic subunit microtubule star (mts), the B regulatory subunit that determines the substrate specificity, and the scaffold protein Pp2A-29B (Figure 7A). Note that in *Drosophila*, there are three forms of the B subunits: widerborst (wdb), twins (tws) and PP2A-B'. Our InsulinNet revealed that the PP2A complex interacts with the core pathway at baseline and 10 minutes, and dissociates at 30 minutes post insulin stimulation. From the InsulinNet-RNAi, we observed that Pp2A-29B knockdown elevates baseline pERK signal and reduces pAkt activity specifically at 30 minutes. From InsulinNet-Phospho, we identified dynamic phosphorylation at Pp2A-29B Ser139, which resides within a consensus motif for Akt1/S6k (RXXS/T). These observations suggest that PP2A modulates insulin signaling, and additionally that feedback regulation by the pathway may serve to downregulate the complex.

To further characterize these interactions, we independently validated interaction between Pp2A-29B and Akt using co-immunoprecipitation and Western blotting (Figure 7B). Further, knocking down Pp2A-29B in cells using independent RNAi reagents increased pS6k activity, whereas overexpressing Pp2A-29B reduces the pS6k levels (Figure 7C). These observation further supports that pS6k is a downstream target of the PP2A complex (Hahn et al., 2010).

Next, we focused on chromatin remodeling complexes, which represent more than 10% of the insulin-associated complexes (15 out of 143). These include the Brahma complex (also called as SWI/SNF complex), which we previously showed to be an essential component of insulin signaling (Vinayagam et al., 2013). Here, we identified a role for the Reptin-Pontin complex (Figure 7D), a subcomplex of the INO80 complex that stably associates with the insulin pathway and positively regulates its activity.

We confirmed the interaction between Reptin, a core member of the Reptin-Pontin complex, and S6kII using co-immunoprecipitation and Western blotting (Figure 7E). Next, we examined the role of the Reptin-Pontin complex in ribosome biogenesis, a key process regulated by Insulin/TOR signaling. In *Drosophila*, ribosomal RNA (rRNA) synthesis, a limiting step of ribosome biogenesis, is induced by the activation of insulin signaling (Figure S4) (Grewal et al., 2005). Consistent with this, inhibiting PI3K (with LY294002) or TOR (with Rapamycin) resulted in decreased rRNA synthesis in *Drosophila* S2R+ cells (Figure 7F). Further, knocking down *reptin* or *pontin* resulted in decreased rRNA synthesis (Figure 7F), suggesting that the Reptin-Pontin complex functions downstream of insulin signaling to regulate rRNA synthesis. Next, we analyzed the role of Reptin-Pontin in regulating nucleolar size, since morphology and size of nucleoli are linked to nucleolar activity (ribosome biogenesis). Strikingly, knocking down *reptin* in S2R+ cells reduces nucleolar size (Figure S5). To query the role of the Reptin-Pontin complex in vivo we examined *Drosophila* larval

muscles, as insulin signaling is required for muscle growth, nuclei and nucleoli size (Demontis and Perrimon, 2009). Overexpressing *InR* using the Dmef2-Gal4 driver in the larval muscle increases nuclei and nucleoli sizes (Figure 7G and Figure S6), whereas knocking down *reptin, pontin*, and *domino* that encodes another member of the Tip60 complex, resulted in smaller muscle fibers and nuclei, and highly disorganized nucleoli (Figure 7G). Altogether, these results confirms that the Reptin-Pontin complex functions downstream of insulin signaling to regulate ribosome biogenesis.

## Discussion

We have built a comprehensive resource of insulin signaling network by systematically identifying network components using three orthogonal datasets generated at three different time points. While small-scale insulin networks have been reported previously (Glatter et al., 2011), our analysis represents the largest and comprehensive resource with dynamics information. Our comparative network analysis showed that the network recapitulates many known interactions of the pathway, and shows significant overlap with relevant networks and importantly identifies several components of insulin network, including a PP2A and Reptin-Pontin complexes. Further, we functionally validated almost half of the network components using RNAi screens and/or phosphoproteomic datasets, demonstrating the high quality and comprehensiveness of this resource.

An important feature of this resource is the integrative framework employed for three orthogonal datasets generated under the same conditions to identify network components. An advantage of such an integrative approach is that it helps to narrow-down high-confidence interactors present in all three datasets. Such integrative approach also enables distinguishing network components that mediate signal propagation, signal integration and feedback regulations. For instance, our comparison of RNAi and phosphoproteomics data sets shows that the proteins that are not hits in RNAi screen are more likely to be regulated by the phosphoproteome. This observation intuitively makes sense, since the RNAi screens identifies nodes that regulate the pathway, whereas the phosphoproteome captures the signal propagation upon stimulation.

Another important feature is the dynamics information associated with the datasets. Our analysis showed that the dynamic information is necessary to capture relevant interactions. For instance the PPI network generated at 10 minutes: 1) identifies many known interactions; 2) shows that the core components of the pathway comes together and shares common interactors; 3) indicates that interacting proteins enriched for functions are more relevant to insulin signaling. Similarly, the hits identified in the 10 minutes RNAi screen significantly overlap with PPIs identified at 10 minutes. Finally, the early-response class phosphosites shows enrichment for Akt/S6k motifs and these phosphoproteins significantly overlap with the PPI dataset. Suggesting the importance of building signaling networks at different time points following stimulation to capture the relevant, dynamic interactions. Although recent phosphoproteomic studies have shown the need for sub-minute temporal resolution to study signaling network dynamics (Kanshin et al., 2015), here we show that the time resolutions chosen in our study capture many functional interactions. This may be due to the heterogeneity within the cell population that helped us to capture some of the early

changes that happens before 10 min of stimulus, or to sustained activity of the pathway. Further, we also observed pERK and pAkt levels reaching peak at 10 min after stimulus suggesting that our data captures the relevant insulin signaling dynamics. Altogether, these examples underscore the richness of information that can be extracted from the data sets we generated and that remain to be explored.

In addition to generating comprehensive datasets, we have established a framework to systematically annotate the insulin network. First, we have organized the complex network into protein complexes. Next, we systematically characterized the activation/inhibition relationships between the complexes and the insulin core-pathway. This annotation framework enabled us to get a global view of how the Insulin core-pathway is interconnected to various cellular machineries and protein complexes. Further, the analysis facilitated the identification of a role for protein complexes such as PP2A and Reptin-pontin in mediating insulin signaling. This annotation framework is more generic and can adapted to other signaling network as well.

Although our insulin network is of highest quality, the false negatives are still an issue. For example, though we used Tsc1 and gig (Tsc2) as baits, we failed to identify CG6182, a *Drosophila* ortholog of TBC1D7, a third component of the Tsc complex (Dibble et al., 2012). In the case of RNAi screens, all six screens put together only validated 47% network components. The remaining 53% non-hits could be due to the: 1) redundancies in the network; 2) false positives in the PPI dataset; or 3) false negatives in the RNAi screens. An independent screen at 60 minutes of insulin stimulus identified an additional proteins as pAkt and/or pERK regulators (data not shown), suggesting that more screens under different time points or more pathway readouts are needed to comprehensively validate the insulin network components. In addition, performing combinatorial perturbations will provide a powerful approach to identify redundancies in the network (Bakal et al., 2008; Fischer et al., 2015; Housden et al., 2015).

In summary, we have generated a comprehensive resource of insulin signaling network. Importantly, we have created InsulinNet (http://fgr.hms.harvard.edu/InsulinNetwork/), to facilitate the query and access InsulinNet-PPI data. Given the conserved nature of the pathway, we expect that this resource will be useful to understand mechanism of human diseases, mine the cancer datasets such as the cancer genome atlas (TCGA), and to identify novel therapeutic targets.

## Experimental Procedures

### Tandem affinity purification data generation and statistical analysis

Briefly, 20 proteins from canonical pathway were used as bait proteins, sub-cloned into the pMK33-CTAP vector and transfected to S2R+ cells. Tandem affinity purification was performed as previously described (Friedman et al., 2011; Kwon et al., 2013). TAP experiments were performed as three independent replicates. All collected MS/MS fragmentation spectra were searched against a dmel-all-translation protein database (FlyBase Consortium) and protein hits were calculated on the basis of the number of reversed database hits above the scoring thresholds. The SAINT algorithm was used to calculate the

probability scores for the interaction between bait and prey observed by MS. More details on experimental procedure and statistical analysis can be found in Supplementary Text.

### RNAi screens

RNAi screening was performed to validate novel components of InsulinNet-PPI as described previously (Friedman and Perrimon, 2006; Friedman et al., 2011; Kockel et al., 2010). Briefly, S2R+ cells were seeded with dsRNAs targeting genes of interest for 72hrs. Cells were stimulated with insulin for 10 or 30 minutes (or not stimulated with insulin for baseline condition), fixed and stained for Akt and ERK activity using In-Cell Western (ICW) Assay. Monoclonal pAkt (Ser505) and pERK (Thr202/Tyr204) antibodies from Cell Signaling technologies were used to quantify the Akt and ERK activities. To define a hit, we computed log2 fold-change value of the phospho-antibody signal of a gene compared to the control as described previously (Friedman and Perrimon, 2006; Friedman et al., 2011; Kockel et al., 2010). Genes with log2 fold-change >= 0.5 are defined as negative regulators and <= −0.5 is defined as positive regulators. Details on experimental procedure and statistical analysis can be found in Supplementary Text.

### Phosphoproteomic analyses

Cells were grown as above for AP-MS experiments, lysed and processing as previously described (Sopko et al., 2014). TMT labeling was as follows: untreated - TMT126; TMT127; 10 minutes insulin - TMT128; TMT129; 30 minutes insulin - TMT130; TMT131. Samples were analyzed on an LTQ OrbiTrap Velos mass spectrometer (Thermo Fisher Scientific) using a data-dependent Top10-MS2 method using (higher-energy collisional dissociation) HCD for reporter ion quantitation. Peptide identification and filtering, and data normalization and phosphosite localization was performed as previously described (Sopko et al., 2014). Details on experimental procedure and statistical analysis can be found in Supplementary Text.

### Computational analysis

Details on computational and statistical analysis correspond to motif enrichment analysis, kinase-substrate prediction, comparative network analysis, GO enrichment analysis and protein complex enrichment analysis can be found on Supplementary Text.

### In vitro and in vivo validations

Details on Co-immunoprecipitation and Western blotting, quantitative real-time RT-PCR and fly stocks and phenotypic analyses can be found on Supplementary Text.

## Supplementary Material

Refer to Web version on PubMed Central for supplementary material.

## Acknowledgments

We thank the Transgenic RNAi Project (TRiP) at Harvard Medical School for flies and the *Drosophila* RNAi Screening Center (Harvard Medical School) for dsRNA amplicons, equipment, and database assistance. The NIH

supported this work (5R01DK088718, 5P01CA120964, 5R01GM084947, and 5R01GM067761). R.S. is a Special Fellow of the Leukemia and Lymphoma Society. N.P. is a Howard Hughes Medical Institute investigator.

## References

Bakal C, Linding R, Llense F, Heffern E, Martin-Blanco E, Pawson T, Perrimon N. Phosphorylation networks regulating JNK activity in diverse genetic backgrounds. Science. 2008; 322:453–456. [PubMed: 18927396]

Boyle EI, Weng S, Gollub J, Jin H, Botstein D, Cherry JM, Sherlock G. GO::TermFinder--open source software for accessing Gene Ontology information and finding significantly enriched Gene Ontology terms associated with a list of genes. Bioinformatics. 2004; 20:3710–3715. [PubMed: 15297299]

Choi H, Larsen B, Lin ZY, Breitkreutz A, Mellacheruvu D, Fermin D, Qin ZS, Tyers M, Gingras AC, Nesvizhskii AI. SAINT: probabilistic scoring of affinity purification-mass spectrometry data. Nat Methods. 2011; 8:70–73. [PubMed: 21131968]

Chou MF, Schwartz D. Biological sequence motif discovery using motif-x. Curr Protoc Bioinformatics Chapter. 2011; 13:15–24. Unit 13.

Clancy DJ, Gems D, Harshman LG, Oldham S, Stocker H, Hafen E, Leevers SJ, Partridge L. Extension of life-span by loss of CHICO, a Drosophila insulin receptor substrate protein. Science. 2001; 292:104–106. [PubMed: 11292874]

Demontis F, Perrimon N. Integration of Insulin receptor/Foxo signaling and dMyc activity during muscle growth regulates body size in Drosophila. Development. 2009; 136:983–993. [PubMed: 19211682]

Dibble CC, Elis W, Menon S, Qin W, Klekota J, Asara JM, Finan PM, Kwiatkowski DJ, Murphy LO, Manning BD. TBC1D7 is a third subunit of the TSC1-TSC2 complex upstream of mTORC1. Mol Cell. 2012; 47:535–546. [PubMed: 22795129]

Fischer B, Sandmann T, Horn T, Billmann M, Chaudhary V, Huber W, Boutros M. A map of directional genetic interactions in a metazoan cell. Elife. 2015:4.

Friedman A, Perrimon N. A functional RNAi screen for regulators of receptor tyrosine kinase and ERK signalling. Nature. 2006; 444:230–234. [PubMed: 17086199]

Friedman AA, Tucker G, Singh R, Yan D, Vinayagam A, Hu Y, Binari R, Hong P, Sun X, Porto M, et al. Proteomic and functional genomic landscape of receptor tyrosine kinase and ras to extracellular signal-regulated kinase signaling. Sci Signal. 2011; 4:rs10. [PubMed: 22028469]

Glatter T, Schittenhelm RB, Rinner O, Roguska K, Wepf A, Junger MA, Kohler K, Jevtov I, Choi H, Schmidt A, et al. Modularity and hormone sensitivity of the Drosophila melanogaster insulin receptor/target of rapamycin interaction proteome. Mol Syst Biol. 2011; 7:547. [PubMed: 22068330]

Grewal SS, Li L, Orian A, Eisenman RN, Edgar BA. Myc-dependent regulation of ribosomal RNA synthesis during Drosophila development. Nat Cell Biol. 2005; 7:295–302. [PubMed: 15723055]

Guruharsha KG, Rual JF, Zhai B, Mintseris J, Vaidya P, Vaidya N, Beekman C, Wong C, Rhee DY, Cenaj O, et al. A protein complex network of Drosophila melanogaster. Cell. 2011; 147:690–703. [PubMed: 22036573]

Hahn K, Miranda M, Francis VA, Vendrell J, Zorzano A, Teleman AA. PP2A regulatory subunit PP2A–B' counteracts S6K phosphorylation. Cell Metab. 2010; 11:438–444. [PubMed: 20444422]

Hopper NA. The adaptor protein soc-1/Gab1 modifies growth factor receptor output in Caenorhabditis elegans. Genetics. 2006; 173:163–175. [PubMed: 16547100]

Housden BE, Valvezan AJ, Kelley C, Sopko R, Hu Y, Roesel C, Lin S, Buckner M, Tao R, Yilmazel B, et al. Identification of potential drug targets for tuberous sclerosis complex by synthetic screens combining CRISPR-based knockouts with RNAi. Sci Signal. 2015; 8:rs9. [PubMed: 26350902]

Hsu PP, Kang SA, Rameseder J, Zhang Y, Ottina KA, Lim D, Peterson TR, Choi Y, Gray NS, Yaffe MB, et al. The mTOR-regulated phosphoproteome reveals a mechanism of mTORC1-mediated inhibition of growth factor signaling. Science. 2011; 332:1317–1322. [PubMed: 21659604]

Humphrey SJ, Azimifar SB, Mann M. High-throughput phosphoproteomics reveals in vivo insulin signaling dynamics. Nat Biotechnol. 2015; 33:990–995. [PubMed: 26280412]

Humphrey SJ, Yang G, Yang P, Fazakerley DJ, Stockli J, Yang JY, James DE. Dynamic adipocyte phosphoproteome reveals that Akt directly regulates mTORC2. Cell Metab. 2013; 17:1009–1020. [PubMed: 23684622]

Kanshin E, Bergeron-Sandoval LP, Isik SS, Thibault P, Michnick SW. A cell-signaling network temporally resolves specific versus promiscuous phosphorylation. Cell Rep. 2015; 10:1202–1214. [PubMed: 25704821]

Kockel L, Kerr KS, Melnick M, Bruckner K, Hebrok M, Perrimon N. Dynamic switch of negative feedback regulation in Drosophila Akt-TOR signaling. PLoS Genet. 2010; 6:e1000990. [PubMed: 20585550]

Kwon Y, Vinayagam A, Sun X, Dephoure N, Gygi SP, Hong P, Perrimon N. The Hippo signaling pathway interactome. Science. 2013; 342:737–740. [PubMed: 24114784]

Miller ML, Jensen LJ, Diella F, Jorgensen C, Tinti M, Li L, Hsiung M, Parker SA, Bordeaux J, Sicheritz-Ponten T, et al. Linear motif atlas for phosphorylation-dependent signaling. Sci Signal. 2008; 1:ra2. [PubMed: 18765831]

Neumuller RA, Gross T, Samsonova AA, Vinayagam A, Buckner M, Founk K, Hu Y, Sharifpoor S, Rosebrock AP, Andrews B, et al. Conserved regulators of nucleolar size revealed by global phenotypic analyses. Sci Signal. 2013; 6:ra70. [PubMed: 23962978]

Reiling JH, Sabatini DM. Stress and mTORture signaling. Oncogene. 2006; 25:6373–6383. [PubMed: 17041623]

Schmidt EE, Pelz O, Buhlmann S, Kerr G, Horn T, Boutros M. GenomeRNAi: a database for cell-based and in vivo RNAi phenotypes, 2013 update. Nucleic Acids Res. 2013; 41:D1021–D1026. [PubMed: 23193271]

Sopko R, Foos M, Vinayagam A, Zhai B, Binari R, Hu Y, Randklev S, Perkins LA, Gygi SP, Perrimon N. Combining genetic perturbations and proteomics to examine kinase-phosphatase networks in Drosophila embryos. Dev Cell. 2014; 31:114–127. [PubMed: 25284370]

Teleman AA. Molecular mechanisms of metabolic regulation by insulin in Drosophila. Biochem J. 2010; 425:13–26. [PubMed: 20001959]

Vinayagam A, Hu Y, Kulkarni M, Roesel C, Sopko R, Mohr SE, Perrimon N. Protein complex-based analysis framework for high-throughput data sets. Sci Signal. 2013; 6:rs5. [PubMed: 23443684]

Vinayagam A, Zirin J, Roesel C, Hu Y, Yilmazel B, Samsonova AA, Neumuller RA, Mohr SE, Perrimon N. Integrating protein-protein interaction networks with phenotypes reveals signs of interactions. Nat Methods. 2014; 11:94–99. [PubMed: 24240319]

White MF. Insulin signaling in health and disease. Science. 2003; 302:1710–1711. [PubMed: 14657487]

Yu Y, Yoon SO, Poulogiannis G, Yang Q, Ma XM, Villen J, Kubica N, Hoffman GR, Cantley LC, Gygi SP, et al. Phosphoproteomic analysis identifies Grb10 as an mTORC1 substrate that negatively regulates insulin signaling. Science. 2011; 332:1322–1326. [PubMed: 21659605]

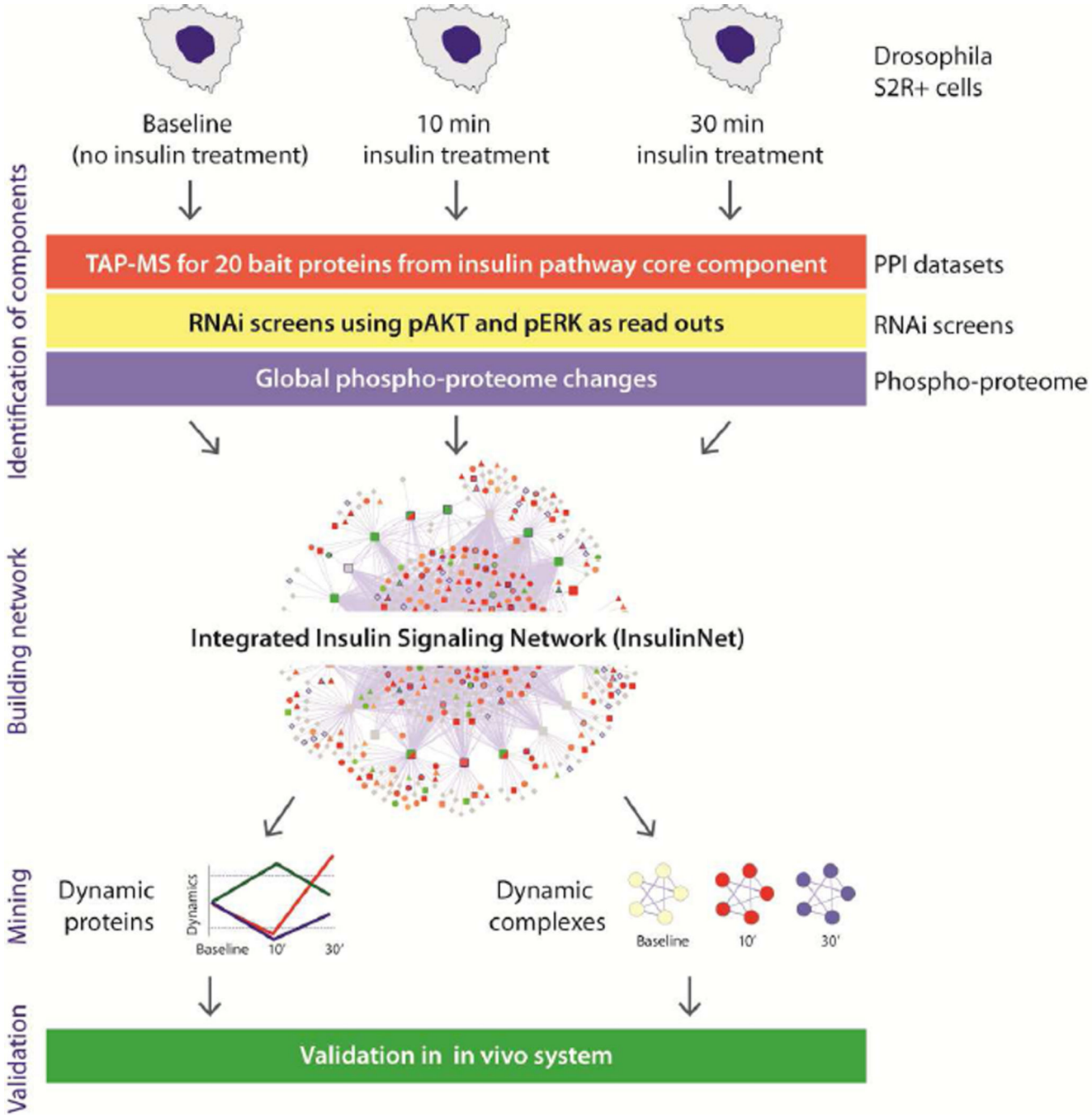


**Figure 1. Overall strategy used to build and mine the *Drosophila* Insulin signaling network**

Three different data sets, protein-protein interaction (PPI), RNAi screens, and phosphoproteomic changes, generated at three different time points (Baseline, 10 minutes and 30 minutes) after insulin stimulation were integrated to build the insulin network (InsulinNet). The network was interrogated to identify dynamic changes at the level of single proteins and protein complexes.

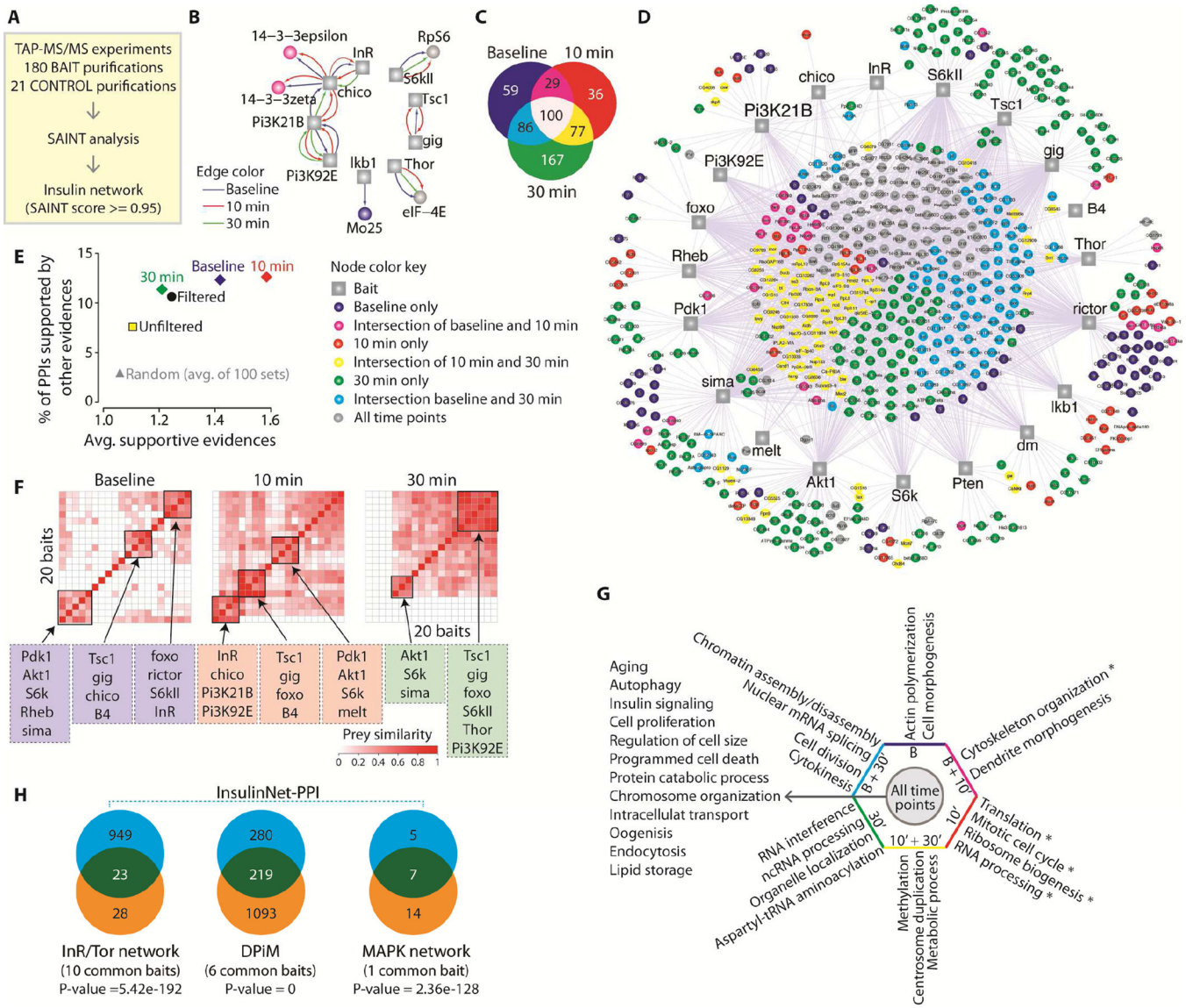


**Figure 2. TAP-MS identification of the PPIs surrounding the *Drosophila* InR/Pi3K/Akt signaling pathway (InsulinNet-PPI)**

**(A)** Overview of the experimental workflow and data processing of the TAP-MS/MS datasets. PPIs were probed for 20 baits in triplicate at three time points (180 TAP-MS/MS experiments). PPIs with a SAINT score ≥0.95 were used to build the network. **(B)** Known canonical interactions recapitulated in the insulin network. Square and circle nodes represent baits and preys, respectively. Edge color represents the time point at which the interaction is identified and the arrow points from the bait to the prey. Node colors are described. **(C)** Venn diagram showing the overlapping prey proteins between the InsulinNet-PPI generated at different time points. **(D)** Integrated insulin network representation of the InsulinNet-PPI surrounding the InR/Pi3K/Akt pathway at three different time points. 20 baits (squares) and 554 preys (circles) are present in the network and connected by 1807 edges. Only PPIs with SAINT score ≥ 0.95 are shown. **(E)** Quality assessment of the InsulinNet-PPI at different time points by comparing with literature curated interactions. **(F)** Clustering the bait proteins

based on the overlapping prey proteins at different time points (see Experimental Procedures for the prey similarity measure). **(G)** Gene Ontology (GO) functional analysis of identified prey proteins (enrichment of biological process terms are shown). B is Baseline. **(H)** Comparison of the InsulinNet-PPI (blue) with other relevant published *Drosophila* PPI datasets (orange). P-value shows the enrichment of overlap compared to randomized networks.

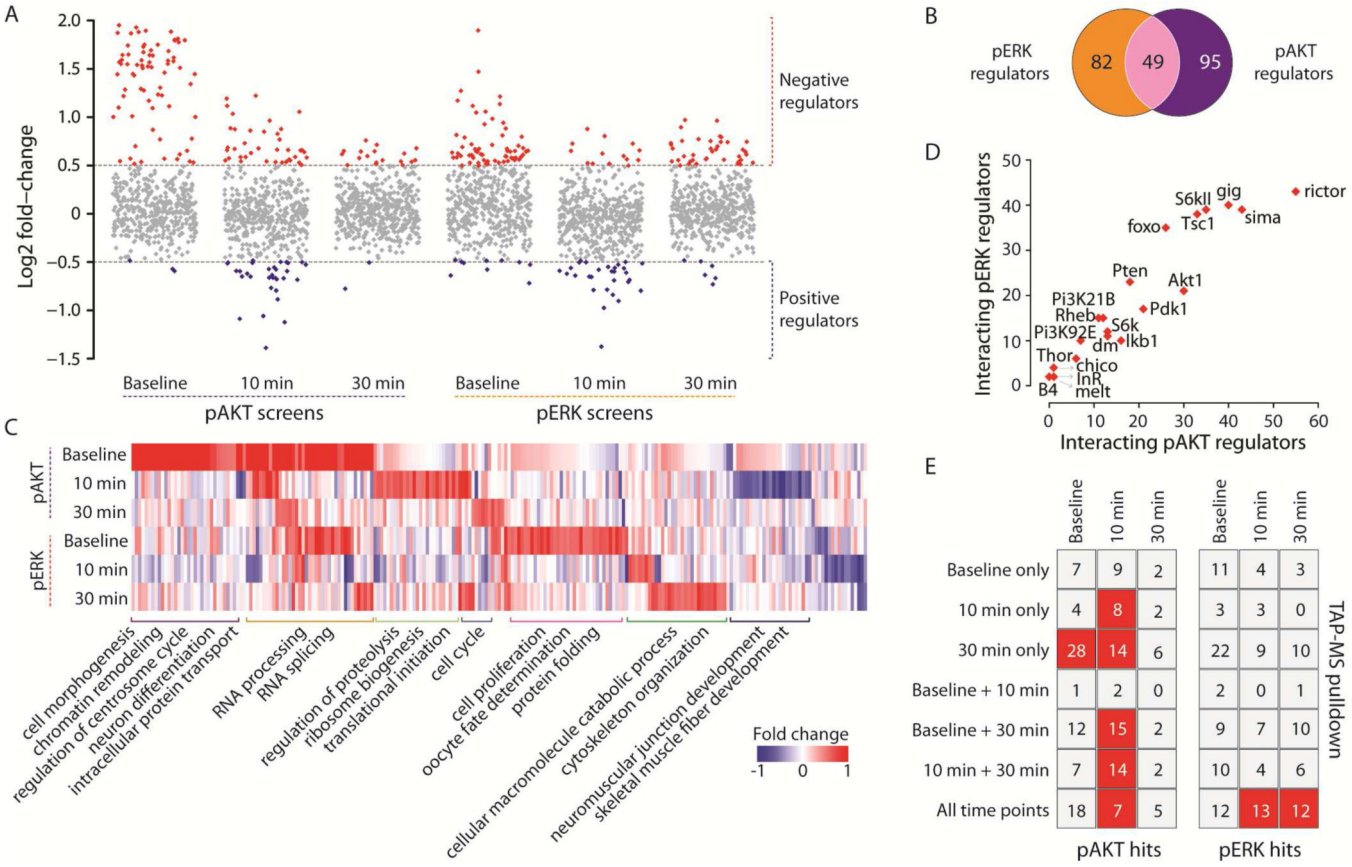


**Figure 3. Functional characterization of the InR/Pi3K/Akt network components using RNAi screens**

**(A)** Plot showing the results from 6 RNAi screens measuring two different readouts (pAkt and pErk) at three different time points (Baseline, 10 minutes and 30 minutes after insulin treatment). The effect of knocking down the prey proteins was tested using RNAi and measured levels of phospho-Akt1 (Ser 479) and dually phosphorylated ERK. Negative and positive regulators of the pathway increase and decrease the phospho-sensors, respectively. **(B)** Venn diagram showing the overlap between pAkt and pErk regulators (all time points have been combined). **(C)** Heat map showing the functional enrichment of pAkt and pErk regulators (GO biological process). **(D)** Plot showing core components of the insulin network according to the number of pERK and pAkt regulators with which they interact. **(E)** Heat map comparing the dynamics of TAP-MS/MS identification vs. the time point at which it regulates the pathway output as monitored by pAkt and pERK. Square filled with red shows that the overlap is significantly enriched compared to the random set.

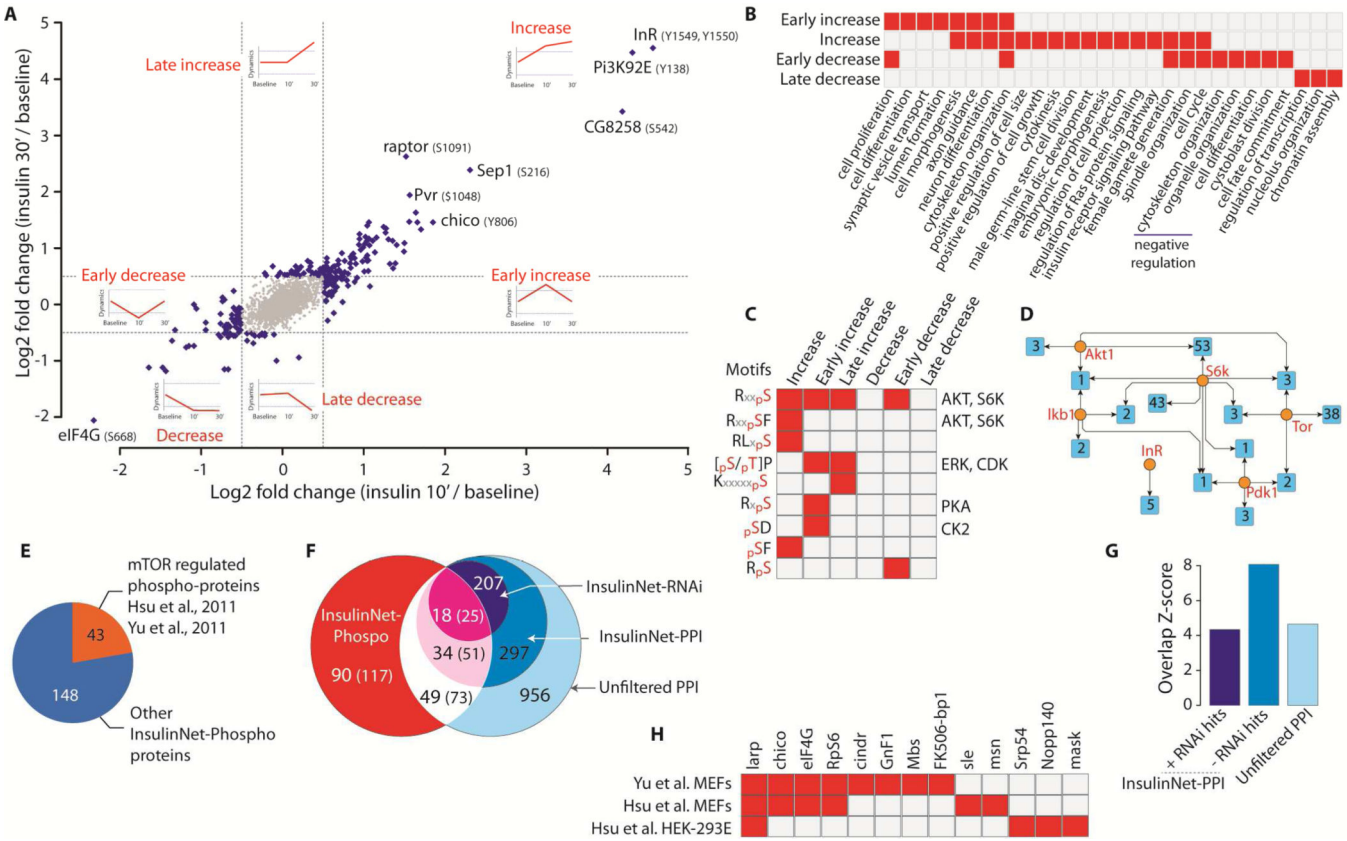


**Figure 4. Dynamically regulated InR/Pi3K/Akt network components identified by quantitative global phosphoproteomics**

**(A)** Scatter plot showing the distinct dynamics of the phosphosites that respond to insulin (InsulinNet-Phospho). Phosphosites are indicated in parenthesis. **(B)** Functional enrichment of the distinct dynamic phosphosites (GO biological process). Boxed filled in red shows significant enrichment and grey otherwise. **(C)** Consensus motifs enriched among the InsulinNet-Phospho proteins. Red filling indicated motif enriched in the given dynamic class. The candidate kinases phosphorylating the sites are indicated. Color code similar to Figure 4B. **(D)** Network picture summarizing the results from Netphorest. Kinases from the core pathway are shown in orange circles and the number of phosphosites with corresponding consensus motifs are shown within the blue nodes. **(E)** Comparative analysis of the InsulinNet-Phospho with mTOR regulated phosphoproteins reported in two previous studies (Hsu et al., 2011; Yu et al., 2011). **(F)** Venn diagram showing the overlap between InsulinNet-PPI, InsulinNet-RNAi and InsulinNet-Phospho. Number in parenthesis indicates phosphosites. **(G)** Enrichment of the overlap correspond to panel **F. (H)** Members of the insulin network phosphorylated in response to insulin previously identified as targets in MEFs and HEK-293E cells (Hsu et al., 2011; Yu et al., 2011). Color code similar to Figure 4B.

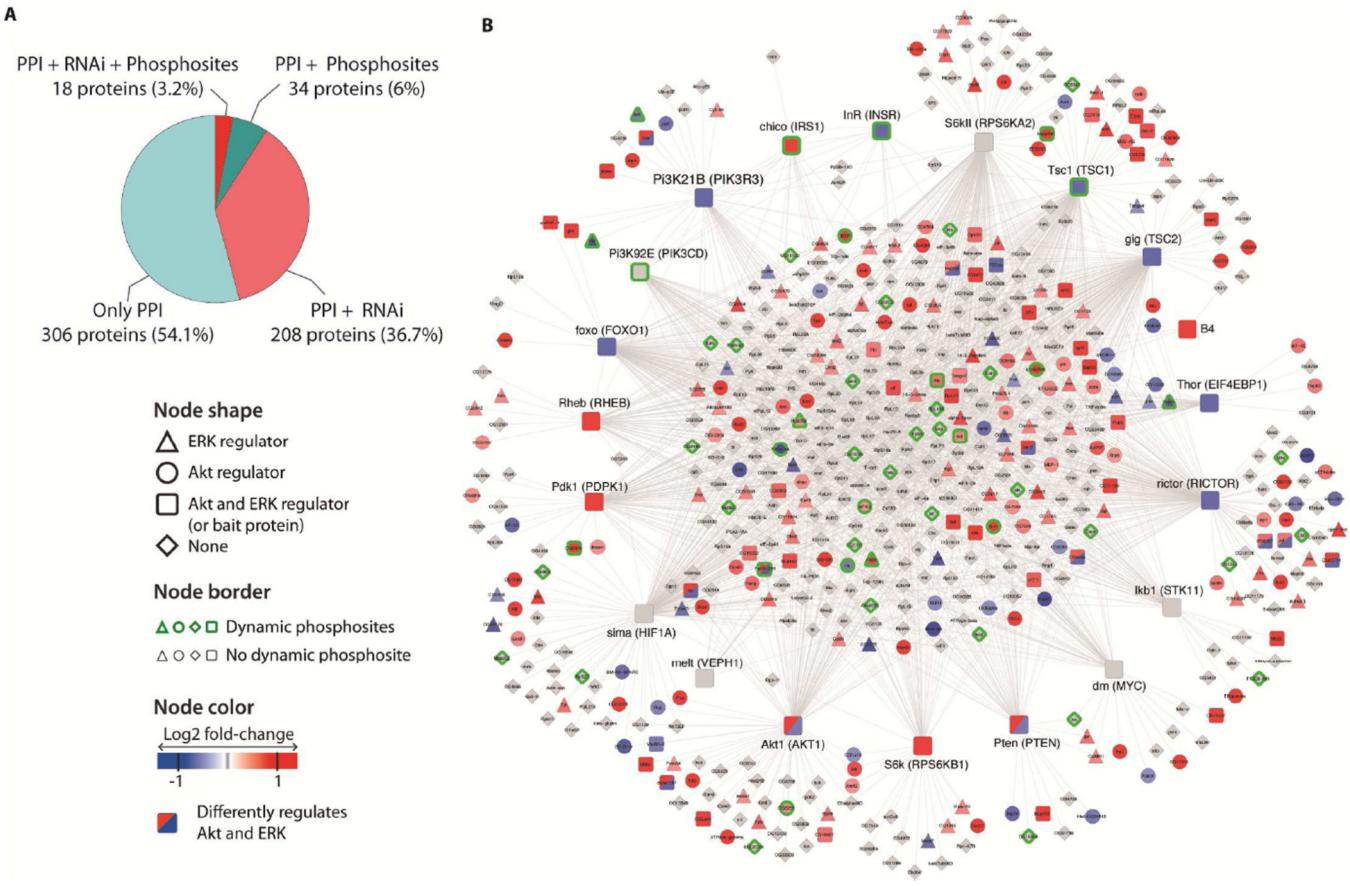


**Figure 5. Integrated *Drosophila* Insulin Signaling Network**

**(A)** Pie chart showing the overlap between, InsulinNet-PPI, InsulinNet-RNAi and InsulinNet-phospho datasets. **(B)** Network view of the InsulinNet, an integrated and functional insulin network.

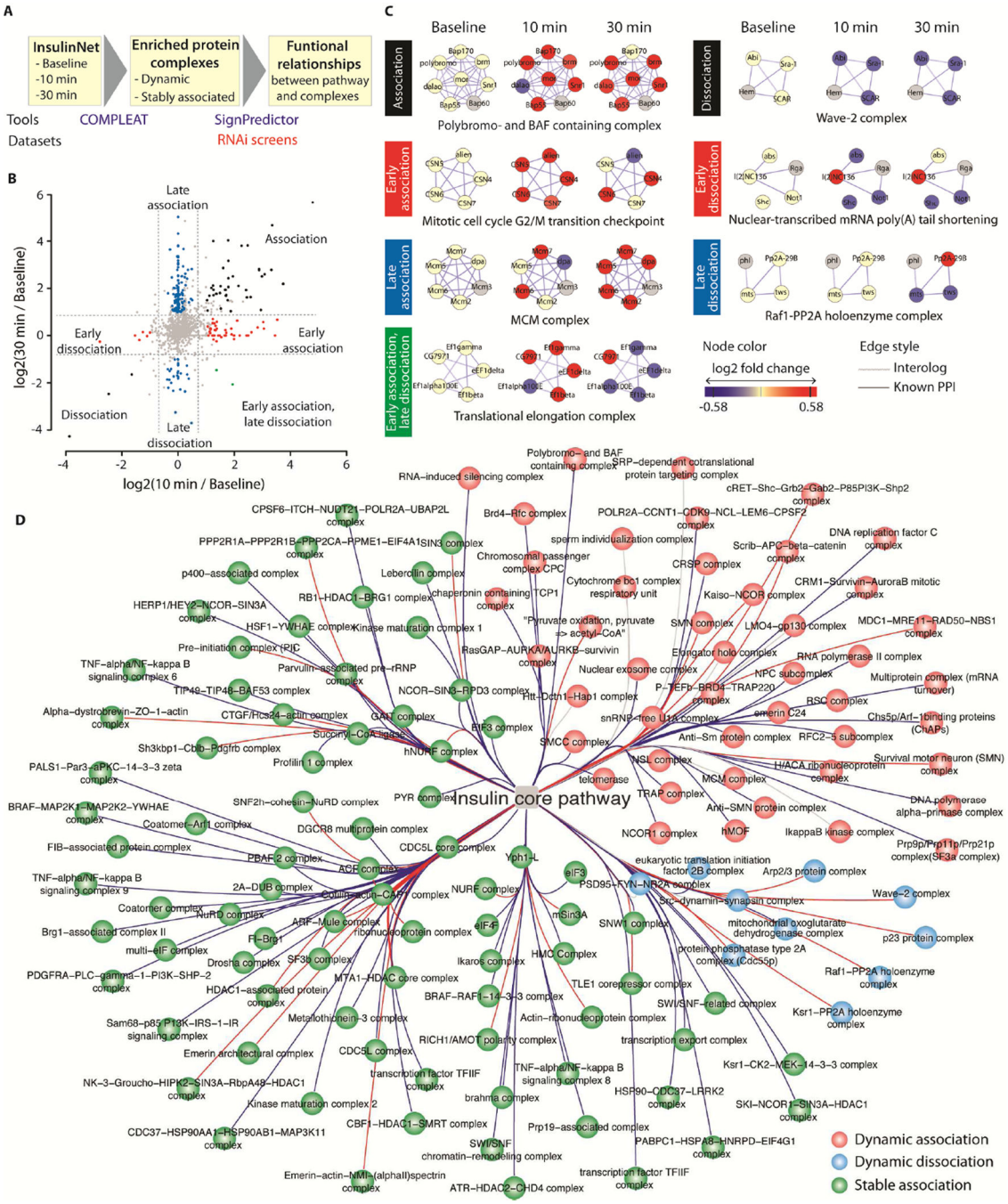


**Figure 6. Protein complex analysis of the insulin network and functional relationships**

**(A)** Flow chart showing the insulin network annotation framework. **(B)** Scatter plot showing the distinct dynamic protein complexes that associate or dissociate with the pathway in response to insulin stimulus. Enriched complexes were identified using the COMPLEAT tool (Vinayagam et al., 2013) and the dynamics is computed based on the InsulinNet-PPI (unfiltered network) (see Experimental Procedures). **(C)** Selected examples of dynamically associating/dissociating protein complexes. **(D)** Protein complex view of the insulin network reconstructed using COMPLEAT and SignPredictor tools. The blue and red edges

correspond to activation and inhibition relationships with the pathway, respectively. Green represents stable associations at all three time points.

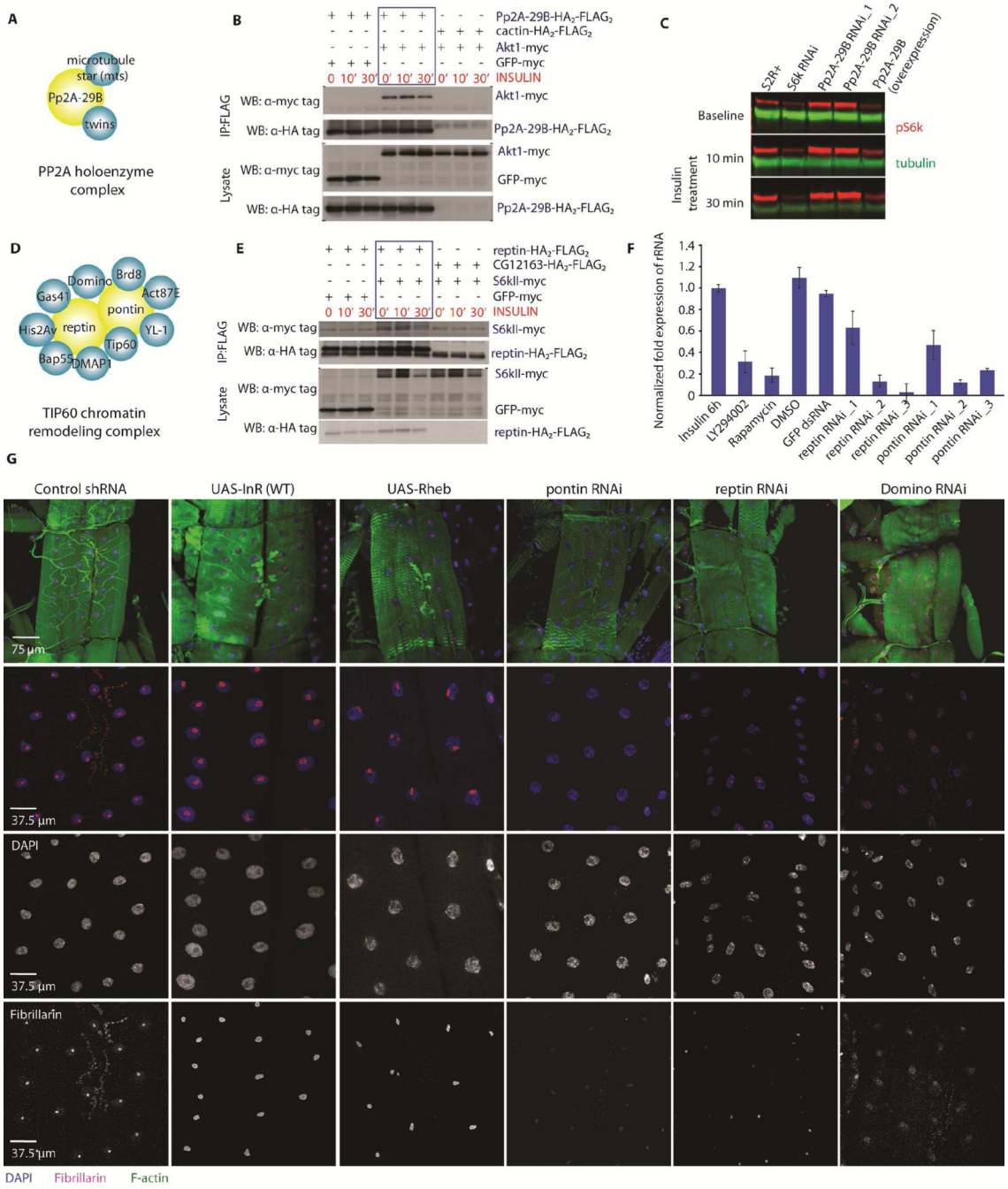


**Figure 7. Functional validation of protein complexes that positively and negatively regulate insulin signaling**

**(A)** Cartoon of the PP2A heterotrimeric holoenzyme complex predicted to act as a negative regulator of the insulin network. **(B)** CoIP validation of the dynamic interaction between the phosphatase subunit Pp2A-29B and Akt1. **(C)** Knocking down *Pp2A-29B* increases phosphorylated S6k (pS6k) levels, while *Pp2A-29B* overexpression reduces pS6k. **(D)** Cartoon of the Tip60 complex, an ATP-dependent chromatin-remodeling complex predicted to positively interact with the insulin network. **(E)** Co-IP validation of the interaction of

Reptin with S6kII. **(F)** Activation of the Insulin pathway induces rRNA synthesis in S2R+ cells. Results are shown 6 hours after insulin stimulation. Note that both LY294002 and Rapamycin, that inhibit PI3K and Tor, respectively, reduce rRNA synthesis. Knockdown of *reptin* or *pontin* results in reduced rRNA synthesis as well (data are shown for three independent RNAi lines each). GFP dsRNA was used as a control. **(G)** Knockdown of *reptin, pontin* and *domino* in *Drosophila* larval muscles results in smaller muscle fibers and nuclei and highly disorganized nucleoli. Note the control shRNA (*Dmef2-Gal4 X UAS-GFP* dsRNA) panel is identical to Figure 4D in Vinayagam et al. (2013) as the experiments in both studies were performed at the same time. Muscles are stained with F-actin, nuclei with DAPI, and nucleoli with anti-Fibrillarin.